An integral formulation for wave propagation on weakly non-uniform potential flows

Simone Mancini[a)], R. Jeremy Astley, Samuel Sinayoko and Gwenael Gabard
Institute of Sound and Vibration Research
University of Southampton
Southampton, United Kingdom - SO17 1BJ

Michel Tournour
Siemens Industry Software NV
Interleuvenlaan 68, Leuven, Belgium - 3001

[a)]e-mail: s.mancini@soton.ac.uk

Abstract

An integral formulation for acoustic radiation in moving flows is presented. It is based on a potential formulation for acoustic radiation on weakly non-uniform subsonic mean flows. This work is motivated by the absence of suitable kernels for wave propagation on non-uniform flow. The integral solution is formulated using a Green's function obtained by combining the Taylor and Lorentz transformations. Although most conventional approaches based on either transform solve the Helmholtz problem in a transformed domain, the current Green's function and associated integral equation are derived in the physical space. A dimensional error analysis is developed to identify the limitations of the current formulation. Numerical applications are performed to assess the accuracy of the integral solution. It is tested as a means of extrapolating a numerical solution available on the outer boundary of a domain to the far field, and as a means of solving scattering problems by rigid surfaces in non-uniform flows. The results show that the error associated with the physical model deteriorates with increasing frequency and mean flow Mach number. However, the error is generated only in the domain where mean flow non-uniformities are significant and is constant in regions where the flow is uniform.

I. INTRODUCTION

Predicting noise radiation from complex sources in moving flows is relevant to the automotive, energy and aeronautical industries. Noise radiation from turbofan nacelles and from other aircraft sources is a problem of particular interest in the aviation sector. Numerical simulation of noise radiation and scattering can significantly reduce costs for design and certification. However, an efficient numerical method for high frequency noise propagation on non-uniform moving flows has not yet been demonstrated. Solving high frequency short wavelength problems on moving flows remains computationally expensive. In the aeronautical industry, noise propagation on non-uniform flows is typically predicted using finite element methods (FEM)[1], discontinuous Galerkin methods (DGM)[2] and high order finite difference schemes[3] .

Although volume based methods, such as FEM, DGM and finite difference schemes are able to solve wave propagation on a non-uniform flow, predicting noise radiation in unbounded domain requires the computational domain to be truncated. The truncation of the domain allows acoustic waves to be damped in a non-physical absorbing zone[3,4,5] and satisfy the radiation condition at the outer boundary of the domain. Moreover, these methods suffer of dispersion error and pollution effects[6]. These features are relevant limitations in case of noise radiation for large-scale short-wavelength problems.

On the other hand, numerical methods based on boundary integral formulations, such as the boundary element method (BEM)[7], inherently satisfy the radiation condition in the kernel and allow wave propagation in unbounded domains to be solved more effectively than in the case of volume based methods. Moreover, the fast multiple BEM (FMBEM) is an efficient algorithm to solve wave radiation and scattering for large-scale short-wavelength problems[8]. However, BEM can only solve wave propagation exactly on uniform mean flows. Extending this method to non-uniform flow regions would be beneficial to a number of applications, such as forward fan noise radiation. A surface integral formulation including non-uniform flow effects would also extend the applicability of wave extrapolation methods. These approaches use an integral formulation defined on a closed surface on which the acoustic field is sampled from an 'inner' domain to radiate the solution to the far field. At the moment these methods are limited to uniform flow[9,10].

Current boundary element modelling practices use the Lorentz transformation[11,12] to solve wave propagation on a uniform mean flow. This variable transformation allows the uniform flow Helmholtz equation to be reduced to the standard Helmholtz problem without approximations. By means of a Lorentz transformation, BEM solvers for the standard Helmholtz equation can therefore be used for wave propagation on uniform flows. However, due to the variable transformation, the physical space is deformed in the

direction of the mean flow. The deformation of the domain complicates the formulation of the boundary conditions and the implementation of the transmission conditions for coupled formulations[13,14]. Alternatively, this drawback can be overcome by using an integral formulation in the physical space as proposed by Wu and Lee[15] in the frequency domain and by Hu[16] in the time domain.

For BEM, only approximate formulations are available for representing non-uniform mean flow effects. Astley and Bain[17] provided an approximate formulation for wave propagation on low Mach number mean flows based on Taylor's transformation[18,19]. In the same work, Astley and Bain[17] reported an error analysis for Taylor's wave equation showing that the accuracy of the physical model depends only upon the mean flow Mach number and the characteristic length scales of the acoustic waves and the mean flow. On the other hand, Tinetti and Dunn[20] provided a generalized local Lorentz transformation to represent the effect of non-uniform mean flows on wave propagation. However, the method has been restricted to mean flow fields with small gradients. Another approach is to move the terms including non-uniform flow effects to the right hand side of the equation and treat them as sources in the domain. The dual-reciprocity method (DRM)[21] is then used to convert the domain integrals into boundary integrals. The absence of a robust method to define interpolating source functions for the DRM restricts the applicability of this approach. Thereby, modeling non-uniform flow effects for BEM is still an open problem.

In this article, we present, in the physical space, an integral formulation with non-uniform flow based on a combination of the physical models associated with the Taylor and Lorentz transformations. The proposed physical model is an approximate formulation of the full linearized potential wave equation for isentropic compressible flows. The integral formulation derived applies to sound radiation on a *weakly non-uniform* potential mean flow. Consider the mean flow as a sum of a uniform and a non-uniform component which vanishes at infinity. The term *weakly non-uniform* indicates that the non-uniform portion of the mean flow is small compared to the uniform part. A free field Green's function is also determined for a subsonic weakly non-uniform flow as a kernel for the integral equation. Moreover, an error analysis is presented to extend and to revisit the estimate provided by Astley and Bain[17]. This analysis shows the dependency of the error related to the physical model on the mean flow Mach number and on the frequency. The proposed formulation will be shown to improve the accuracy of the model compared to existing formulations based on either Taylor or Lorentz transforms being applied separately.

The paper is structured as follows. Section II presents the physical models. In Section III integral formulations are derived for wave propagation on weakly non-uniform mean flows and the Taylor formulation in the physical space. The Green's functions associated with the integral formulations are derived in Sec. IV and a variational statement

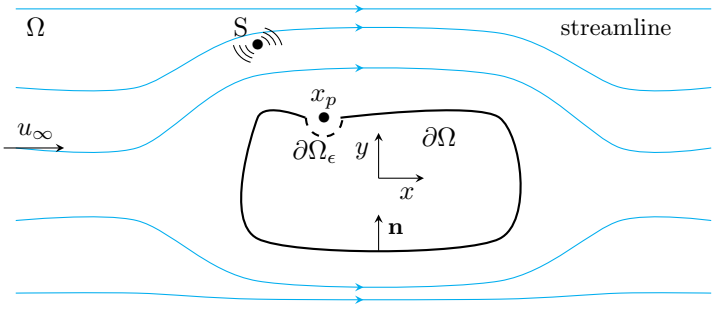

Figure 1: Schematic diagram of the reference problem showing mean flow streamlines in the solution domain Ω.

of the integral equations is given in Sec. V for an arbitrary source distribution. In Sec. VI, a dimensional error analysis is developed to describe the limitation of the proposed solutions. Finally, in Sec. VII some numerical results are presented to benchmark the integral formulations.

II. PHYSICAL MODEL

A numerical solution to external noise radiation and scattering of a source S in a domain Ω by a body $\partial\Omega$ in a non-uniform potential subsonic mean flow is sought (see Fig. 1). Consider an inviscid, adiabatic and irrotational flow and assume that acoustic perturbations are of small amplitude compared with the steady mean flow. Under these hypotheses, wave propagation on a non-uniform mean flow can be described by means of a potential formulation[22] as,

$$\frac{D_0}{Dt}\left(\frac{\rho_0}{c_0^2}\frac{D_0\hat{\phi}}{Dt}\right) - \boldsymbol{\nabla}\cdot\left(\rho_0\boldsymbol{\nabla}\hat{\phi}\right) = 0 \tag{1}$$

where $\hat{\phi}$ is the acoustic velocity potential and $D_0/Dt = \partial/\partial t + \mathbf{u}_0\cdot\nabla$ denotes the material derivative over the mean flow; ρ_0 is the mean flow density, c_0 the speed of sound and $\mathbf{u}_0$ the mean flow velocity. Consider Bernoulli's equation

$$c_0^2 = c_\infty^2 - \frac{\gamma-1}{2}(\|\mathbf{u}_0\|^2 - \|\mathbf{u}_\infty\|^2) \tag{2}$$

where c_∞ and $\mathbf{u}_\infty$ are the speed of sound and the mean flow velocity vector in the far field. By means of Eqs. (2) and introducing the state equation,

$$\frac{d\rho_0}{\rho_0} = \frac{\gamma-1}{2}\frac{dc_0^2}{c_0^2}, \tag{3}$$

Eq. (1) reduces to:

$$\begin{aligned}\frac{\partial^2\hat{\phi}}{\partial t^2}+2\mathbf{u}_0\cdot\boldsymbol{\nabla}\frac{\partial\hat{\phi}}{\partial t} - c_\infty^2\nabla^2\hat{\phi} + \mathbf{u}_0\cdot\boldsymbol{\nabla}(\mathbf{u}_0\cdot\boldsymbol{\nabla}\hat{\phi}) \\ + \frac{1}{2}\boldsymbol{\nabla}\hat{\phi}\cdot\boldsymbol{\nabla}(\mathbf{u}_0\cdot\mathbf{u}_0) + (\gamma-1)\frac{D_0\hat{\phi}}{Dt}\boldsymbol{\nabla}\cdot\mathbf{u}_0 \\ + \frac{\gamma-1}{2}(\|\mathbf{u}_0\|^2 - \|\mathbf{u}_\infty\|^2)\nabla^2\hat{\phi} = 0.\end{aligned} \tag{4}$$

Equation (1) is rewritten as Eq. (4) to allow a dimensional analysis to be performed. Mayoral and Papamoschou[23], following Astley and Bain[17], have provided a description of the dependency of the terms in Eq. (4) on the mean flow Mach number $M_\infty = u_\infty/c_\infty$, the acoustic characteristic length scale L_A and the characteristic length scale of the mean flow L_M. On this basis, Eq. (4) is simplified by retaining only terms of order $[\phi]/L_A^2$, $M_\infty[\phi]/L_A^2$, $M_\infty^2[\phi]/L_A^2$, assuming that $L_A \leq L_M$ and $M_\infty \ll 1$,

$$\begin{aligned}\frac{\partial^2\hat{\phi}}{\partial t^2}+2\mathbf{u}_0\cdot\boldsymbol{\nabla}\frac{\partial\hat{\phi}}{\partial t} - c_\infty^2\nabla^2\hat{\phi} + \mathbf{u}_0\cdot\boldsymbol{\nabla}(\mathbf{u}_0\cdot\boldsymbol{\nabla}\hat{\phi}) \\ + \frac{1}{2}\boldsymbol{\nabla}\hat{\phi}\cdot\boldsymbol{\nabla}(\mathbf{u}_0\cdot\mathbf{u}_0) + \frac{\gamma-1}{2}(\|\mathbf{u}_0\|^2 - \|\mathbf{u}_\infty\|^2)\nabla^2\hat{\phi} = 0.\end{aligned} \tag{5}$$

Consider the mean flow formed by a uniform component $\mathbf{u}_\infty$ and a non-uniform portion $\mathbf{u}_0'$. The main idea is to consider only first order effects in $\mathbf{u}_0'$ over wave convection due to $\mathbf{u}_\infty$. If $\mathbf{u}_0 = \mathbf{u}_\infty + \mathbf{u}_0'$, where $\|\mathbf{u}_0'\| \ll \|\mathbf{u}_\infty\|$ and if it is assumed that the uniform mean flow velocity $\mathbf{u}_\infty$ is aligned with the positive x-axis, Eq. (5) reduces to:

$$\frac{\partial^2\hat{\phi}}{\partial t^2} + 2\mathbf{u}_0\cdot\boldsymbol{\nabla}\frac{\partial\hat{\phi}}{\partial t} - c_\infty^2\nabla^2\hat{\phi} + u_\infty^2\frac{\partial^2\hat{\phi}}{\partial x^2} = 0. \tag{6}$$

Hereafter, Eq. (6) is referred to as the wave equation for *weakly non-uniform* potential flow.

In the case of a uniform flow, where $\mathbf{u}_0 \equiv \mathbf{u}_\infty$ at all points in the flow, Eq. (6) reduces to the uniform flow wave equation without approximation,

$$\left(\frac{\partial}{\partial t} + u_\infty\frac{\partial}{\partial x}\right)^2\hat{\phi} - c_\infty^2\nabla^2\hat{\phi} = 0. \tag{7}$$

If the mean flow is uniform, solutions of Eq. (7) are also solution of Eq. (1) without approximation. On the other hand, if terms of the order M_∞^2 are neglected in Eq. (6), it reduces to

$$\frac{\partial^2 \hat{\phi}}{\partial t^2} + 2\mathbf{u}_0 \cdot \boldsymbol{\nabla} \frac{\partial \hat{\phi}}{\partial t} - c_\infty^2 \nabla^2 \hat{\phi} = 0. \tag{8}$$

In all that follows, Equation (8) is referred to as the *Taylor wave equation*, because it is consistent with the solution based on the Taylor transformation[17,18]. It is an approximation of order M_∞ of Eq. (1) accounting for a non-uniform mean flow.

If a time harmonic problem in which all perturbed quantities varies as $\mathrm{e}^{\mathrm{i}\omega t}$ is considered, the acoustic velocity potential in the frequency domain can be defined as $\hat{\phi} = \phi e^{\mathrm{i}\omega t}$ where ϕ is a complex amplitude. In the Fourier domain Eqs. (6), (7) and (8) are respectively referred to as the *weakly non-uniform potential flow Helmholtz equation*, the *uniform flow Helmholtz equation* and the *Taylor-Helmholtz equation*.

III. BOUNDARY INTEGRAL FORMULATION

A. Weakly non-uniform potential flow Helmholtz equation

By assuming a harmonic time dependence for $\hat{\phi}$, Eq. (6) can be rewritten

$$k^2\phi - 2\mathrm{i}k\mathbf{M}_0 \cdot \boldsymbol{\nabla}\phi + \nabla^2\phi - M_\infty^2 \frac{\partial^2 \phi}{\partial x^2} = 0, \tag{9}$$

where $\mathbf{M}_0$ is the mean flow Mach number vector, $k = \omega/c_\infty$, and M_∞ is the uniform flow Mach number, provided that $\mathbf{M}_\infty = (M_\infty, 0, 0)$. First, the reverse flow operator associated with Eq. (9) is defined considering a mean flow in the opposite direction of the actual flow field, as

$$k^2\phi + 2ik\mathbf{M}_0 \cdot \boldsymbol{\nabla}\phi + \nabla^2\phi - M_\infty^2 \frac{\partial^2 \phi}{\partial x^2} = 0. \tag{10}$$

Following the general approach of Wu and Lee[15], a Green's function G for the fundamental reverse flow operator Eq. (10) is derived

$$k^2 G + 2\mathrm{i}k\mathbf{M}_0 \cdot \boldsymbol{\nabla} G + \nabla^2 G - M_\infty^2 \frac{\partial^2 G}{\partial x^2} = -\delta(\mathbf{x}_p - \mathbf{x}_s), \tag{11}$$

where $\mathbf{x}_p$ is an arbitrary field point, $\mathbf{x}_s$ denotes the point source location and δ is the Dirac delta function. The Green's function G represents the effect of a point source in a non-uniform flow whose direction is opposite to the actual base flow. G therefore differs from the Green's function of the direct fundamental operator and is derived in Sec. IV.

To obtain an integral formulation for the weakly non-uniform potential flow Helmholtz equation, Eq. (9) is multiplied by G and Eq. (11) by ϕ. Subtracting these two equations and integrating over the domain Ω yields

$$\begin{aligned}
&\int_\Omega \phi \left(k^2 G + 2\mathrm{i}k\mathbf{M}_0 \cdot \boldsymbol{\nabla} G + \nabla^2 G - M_\infty^2 \frac{\partial^2 G}{\partial x^2} \right) dV \\
&- \int_\Omega G \left(k^2 \phi - 2\mathrm{i}k\mathbf{M}_0 \cdot \boldsymbol{\nabla} \phi + \nabla^2 \phi - M_\infty^2 \frac{\partial^2 \phi}{\partial x^2} \right) dV \\
&= - \int_\Omega \phi \delta(\mathbf{x}_p - \mathbf{x}_s) dV.
\end{aligned} \tag{12}$$

The divergence theorem is applied to the l.h.s. of Eq. (12) in order to obtain an integral on the boundary surface of the domain $\partial\Omega$. Consistent with the assumptions already made in the derivation of Eq. (6), some terms of higher order in M_∞ will be neglected. Consider the linear term in $\mathbf{M}_0$ in Eq. (12),

$$\begin{aligned}
&\int_\Omega (2\mathrm{i}k\phi\mathbf{M}_0 \cdot \boldsymbol{\nabla} G + 2ikG\mathbf{M}_0 \cdot \boldsymbol{\nabla}\phi) dV \\
&= \int_\Omega 2\mathrm{i}k[\boldsymbol{\nabla} \cdot (\mathbf{M}_0 G\phi) - G\phi \boldsymbol{\nabla} \cdot \mathbf{M}_0] dV.
\end{aligned} \tag{13}$$

Since[17]

$$\nabla \cdot \mathbf{M}_0 = \frac{\frac{1}{2}\mathbf{M}_0 \cdot \boldsymbol{\nabla}(\mathbf{M}_0 \cdot \mathbf{M}_0)}{1 - \frac{\gamma-1}{2}(M_0^2 - M_\infty^2)}, \tag{14}$$

where $M_0 = \|\mathbf{M}_0\|$, is of the same order as M_∞^3, and since high order terms in M_∞ have already been neglected in Eq. (6), the second term on the r.h.s of Eq. (13) can be dropped, giving

$$\int_\Omega 2\mathrm{i}k[\boldsymbol{\nabla} \cdot (\mathbf{M}_0 G\phi) - G\phi \boldsymbol{\nabla} \cdot \mathbf{M}_0] dV \simeq \int_{\partial\Omega} 2\mathrm{i}k\mathbf{M}_0 \cdot \mathbf{n} G\phi dS, \tag{15}$$

where $\mathbf{n}$ is the normal unit vector to $\partial\Omega$ (see Fig. 1). Hence, Eq. (12) can then be rewritten as

$$\begin{aligned}
\phi(\mathbf{x}_p) = &\int_{\partial\Omega} \left[G\frac{\partial\phi}{\partial n} - \phi\frac{\partial G}{\partial n} \right] dS \\
&- \int_{\partial\Omega} \left[2\mathrm{i}k\mathbf{M}_0 \cdot \mathbf{n} G\phi + M_\infty^2 \left(G\frac{\partial\phi}{\partial x} - \phi\frac{\partial G}{\partial x} \right) n_x \right] dS,
\end{aligned} \tag{16}$$

where n_x is the $x-$component of the normal vector to the boundary surface. As shown by Wu and Lee[15] the contribution of the boundary integral at infinity is zero provided that ϕ and G satisfy the Sommerfeld radiation condition with flow.

Equation (16) applies to any point $\mathbf{x}_p$ internal to the domain Ω. On the other hand, for any point on the boundary surface $\partial\Omega$, a limit approach[7] should be used to overcome the singularity of the integral formulation, which is integrable in the sense of Cauchy's principal value. The following equation extends the uniform flow solution of Wu and Lee[15] and is derived in Appendix A,

$$\begin{aligned}\hat{C}(\mathbf{x}_p)\phi(\mathbf{x}_p) = &\int_{\partial\Omega}\left[G\frac{\partial\phi}{\partial n} - \phi\frac{\partial G}{\partial n}\right]dS \\ &- \int_{\partial\Omega}\left[2\mathrm{i}k\mathbf{M}_0\cdot\mathbf{n}G\phi + M_\infty^2\left(G\frac{\partial\phi}{\partial x} - \phi\frac{\partial G}{\partial x}\right)n_x\right]dS,\end{aligned} \tag{17}$$

where

$$\hat{C}(\mathbf{x}_p) = \begin{cases} 1 & \mathbf{x}_p \in \Omega \\ 1 - \int_{\partial\Omega}\left(\frac{\partial G_0}{\partial n} - M_\infty^2\frac{\partial G_0}{\partial x}n_x\right)dS & \mathbf{x}_p \in \partial\Omega \end{cases} \tag{18}$$

In summary, Eq. (17) provides a boundary integral formulation for wave propagation on weakly non-uniform potential mean flows. It models first order non-uniform mean flow effects on wave propagation. The accuracy of the formulation depends on the deviation of the non-uniform flow $\mathbf{M}_0'$ on the uniform component $\mathbf{M}_\infty$. Equation (17) is exact for wave propagation over a uniform mean flow and equivalent to the formulation presented by Wu and Lee[15] for a uniform flow. It reduces to the standard Helmholtz integral equation as $M_0 \to 0$.

B. Taylor-Helmholtz equation

For the Taylor-Helmholtz equation,

$$k^2\phi - 2\mathrm{i}k\mathbf{M}_0\cdot\boldsymbol{\nabla}\phi + \nabla^2\phi = 0, \tag{19}$$

an integral solution in the frequency domain is sought. The Green's function for the reverse flow operator associated with the above equation is denoted by G_T, where

$$k^2G_T + 2\mathrm{i}k\mathbf{M}_0\cdot\boldsymbol{\nabla}G_T + \nabla^2G_T = -\delta(\mathbf{x}_p - \mathbf{x}_s). \tag{20}$$

G_T differs from G and is derived subsequently in Sec. IV using a different set of assumptions consistent with a solution in the Taylor transformed space.

Equation (19) is obtained from Eq. (9) assuming $M_\infty^2 \ll 1$ and $L_A \leq L_M$. Hence, with the same assumptions, the integral solution to Eq. (19) is derived from Eq. (16) by dropping the terms of order M_∞^2 giving

$$\phi(\mathbf{x}_p) = \int_{\partial\Omega}\left(G_T\frac{\partial\phi}{\partial n} - \phi\frac{\partial G_T}{\partial n} - 2\mathrm{i}k\mathbf{M}_0\cdot\mathbf{n}G_T\phi\right)dS. \tag{21}$$

Equation (21) is written for a generic point internal to the domain Ω. However, the integral becomes singular on the boundary surface[7] $\partial\Omega$. On $\partial\Omega$ the singularity is integrable in the sense of the Cauchy's principal value.

Following the procedure showed in Appendix A, a limit approach to the boundary surface is performed. In this case, the static operator associated to Eq. (20) is the Laplacian, $\nabla^2 G_{0_T} = 0$. The static operator is the same as for the standard Helmholtz problem. Therefore, the Cauchy principal value integral, obtained in this case, is the same as for the standard Helmholtz equation[7]. By defining

$$C(\mathbf{x}_p) = \begin{cases} 1 & \mathbf{x}_p \in \Omega \\ 1 - \int_{\partial\Omega} \frac{\partial G_{0_T}}{\partial n} dS & \mathbf{x}_p \in \partial\Omega \end{cases} \tag{22}$$

where $G_{0_T} = 1/(4\pi R)$ and R is the distance between the source and the observer, the following integral solution is obtained,

$$C(\mathbf{x}_p)\phi(\mathbf{x}_p) = \int_{\partial\Omega} \left(G_T \frac{\partial \phi}{\partial n} - \phi \frac{\partial G_T}{\partial n} - 2\mathrm{i}k\mathbf{M}_0 \cdot \mathbf{n} G_T \phi \right) dS. \tag{23}$$

IV. GREEN'S FUNCTION FOR WEAKLY NON-UNIFORM MEAN FLOWS

The Green's function of the reverse flow operator, Eq. (11), is derived by means of a variable transformation. To determine G, a Taylor transformation[18] is applied following a Lorentz transformation[11] of the fundamental reverse flow problem,

$$\frac{\partial^2 \hat{G}}{\partial t^2} - 2\mathbf{u}_0 \cdot \boldsymbol{\nabla} \frac{\partial \hat{G}}{\partial t} - c_\infty^2 \nabla^2 \hat{G} + u_\infty^2 \frac{\partial^2 \hat{G}}{\partial x^2} = c_\infty^2 \delta(\mathbf{x}, t), \tag{24}$$

where $\hat{G} = G\mathrm{e}^{\mathrm{i}\omega t}$. In the Taylor-Lorentz space, Eq. (24) reduces to the standard Helmholtz problem. Since the fundamental solution of the Helmholtz operator is well-known[7], the Green's function in the physical space, G, is retrieved by applying the inverse Taylor-Lorentz transformation to the Green's function in the transformed domain.

Consider first a Lorentz transformation[11] corresponding to a uniform mean flow in the direction opposite to the x-axis, such that the independent variables are transformed as follows:

$$X = \frac{x}{\beta_\infty}, \quad Y = y, \quad Z = z, \quad T = t\beta_\infty - \frac{M_\infty x}{c_\infty \beta_\infty} \tag{25}$$

where $\mathbf{X} = (X, Y, Z)$ and T denote the space and time coordinates in the Lorentz space, whereas (x, y, z, t) denotes the physical space-time domain coordinates and $\beta_\infty = \sqrt{1 - M_\infty^2}$. The differential operators transform as:

$$\begin{aligned} \frac{\partial}{\partial t} =& \beta_\infty \frac{\partial}{\partial T}, \\ \frac{\partial}{\partial x} = \frac{1}{\beta_\infty}\frac{\partial}{\partial X} - \frac{M_\infty}{c_\infty}\frac{1}{\beta_\infty}\frac{\partial}{\partial T}, \qquad & \frac{\partial}{\partial y} = \frac{\partial}{\partial Y}, \qquad \frac{\partial}{\partial z} = \frac{\partial}{\partial Z}. \end{aligned} \tag{26}$$

The Lorentz transformation is applied to Eq. (24) in which $\mathbf{M}_0(\mathbf{x}) = \mathbf{M}_\infty + \mathbf{M}_0'(\mathbf{x})$. This gives

$$\frac{\partial^2 \hat{G}}{\partial T^2} - c_\infty^2 \nabla_X^2 \hat{G} - 2c_\infty \mathbf{M}_0' \cdot \frac{\partial}{\partial T}\left(\boldsymbol{\nabla}_X \hat{G} - \frac{\mathbf{M}_\infty}{c_\infty}\frac{\partial \hat{G}}{\partial T}\right) = c_\infty^2 \delta(\mathbf{X}, T). \tag{27}$$

Note that the Lorentz transformation converts the convected wave equation on a uniform flow ($M_0' = 0$) into the standard wave equation. In the case of a weakly non-uniform mean flow ($M_0' \neq 0$), it introduces an extra term associated with the mean flow variations. Since $M_\infty M_0' \ll M_\infty^2$, as assumed in Eq. (6), Eq. (27) can be approximated by

$$\frac{\partial^2 \hat{G}}{\partial T^2} - c_\infty^2 \nabla_X^2 \hat{G} - 2c_\infty \mathbf{M}_0' \cdot \frac{\partial \boldsymbol{\nabla}_X \hat{G}}{\partial T} = c_\infty^2 \delta(\mathbf{X}, T). \tag{28}$$

A Taylor transformation[18] is now applied to Eq. (28) also considering a non-uniform mean flow component opposite to the actual base flow. The independent variables can be rewritten in the Taylor space as follows:

$$\tilde{X} = X, \quad \tilde{Y} = Y, \quad \tilde{Z} = Z, \quad \tilde{T} = T - \frac{\Phi_0'(\mathbf{X})}{c_\infty^2} \tag{29}$$

where $\Phi_0'(\mathbf{X})$ is the mean flow velocity potential corresponding to $\mathbf{M}_0'$, $\tilde{\mathbf{X}} = (\tilde{X}, \tilde{Y}, \tilde{Z})$ and $\tilde{T}$ denote the Taylor-Lorentz space-time. Differential operators in the Taylor space are given by

$$\frac{\partial}{\partial T} = \frac{\partial}{\partial \tilde{T}}, \quad \boldsymbol{\nabla}_X = \boldsymbol{\nabla}_{\tilde{X}} - \frac{\mathbf{M}_0'}{c_\infty}\frac{\partial}{\partial \tilde{T}}. \tag{30}$$

Equation (28) can then be rewritten as,

$$\frac{\partial^2 \hat{G}}{\partial \tilde{T}^2} - c_\infty^2 \left[\nabla_{\tilde{X}}^2 \hat{G} - 2\left(\boldsymbol{\nabla}_{\tilde{X}} \cdot \frac{\mathbf{M}_0'}{c_\infty}\right)\frac{\partial \hat{G}}{\partial \tilde{T}} - \frac{\|\mathbf{M}_0'\|^2}{c_\infty^2}\frac{\partial^2 \hat{G}}{\partial \tilde{T}^2}\right] = c_\infty^2 \delta(\tilde{\mathbf{X}}, \tilde{T}) \tag{31}$$

Noticing that $\nabla \cdot \mathbf{M}_0'$ is of order M_∞^3 (see Eq. (14)) and neglecting higher order terms in M_0', Eq. (31) yields

$$\frac{\partial^2 \hat{G}}{\partial \tilde{T}^2} - c_\infty^2 \nabla_{\tilde{X}}^2 \hat{G} = c_\infty^2 \delta(\tilde{\mathbf{X}}, \tilde{T}). \tag{32}$$

The l.h.s. of the above equation is the standard wave operator in the Taylor-Lorentz space and is independent of the mean flow.

Since a steady state problem is considered, Eq. (32) is transformed to the frequency domain. The Lorentz transformation introduces a time contraction defined by the factor β_∞ which, in turn, becomes a frequency dilation. In particular, the angular frequency in the Taylor-Lorentz space is $\tilde{\omega} = \omega/\beta_\infty$. The Taylor transformation introduces only a time delay. Therefore, Eq (32) is rewritten as,

$$\tilde{k}^2 G + \nabla_{\tilde{X}}^2 G = -\delta(\tilde{\mathbf{X}}), \tag{33}$$

where $\tilde{k} = \tilde{\omega}/c_\infty$. For free field boundary conditions, the solution of Eq. (33), given by the monopole source solution, is

$$G(\tilde{\mathbf{X}}) = \frac{1}{\beta_\infty} \frac{\mathrm{e}^{-\mathrm{i}\tilde{k}\tilde{R}}}{4\pi\tilde{R}} \tag{34}$$

where $\tilde{R} = \sqrt{\tilde{X}^2 + \tilde{Y}^2 + \tilde{Z}^2}$.

Equation (34) is reformulated in the physical space, where a harmonic solution $G(\mathbf{x}, t) = \bar{G}(\mathbf{x})\mathrm{e}^{\mathrm{i}\omega t}$ is sought. An equivalent harmonic solution in the Taylor-Lorentz space is given by $G(\tilde{\mathbf{X}}, \tilde{T}) = G(\tilde{\mathbf{X}})\mathrm{e}^{\mathrm{i}\tilde{\omega}\tilde{T}}$. Applying the inverse Taylor-Lorentz transformation to the independent variables in $G(\tilde{\mathbf{X}}, \tilde{T})$ yields

$$G(\tilde{\mathbf{X}})\mathrm{e}^{\mathrm{i}\tilde{\omega}\tilde{T}} = \bar{G}(\mathbf{x})\exp\left[\mathrm{i}\frac{\omega}{\beta_\infty}\left(\beta_\infty t - \frac{M_\infty x}{c_\infty \beta_\infty} - \beta_\infty \frac{\Phi_0'(\mathbf{x})}{c_\infty^2}\right)\right] = G(\mathbf{x})\mathrm{e}^{\mathrm{i}\omega t} \tag{35}$$

where

$$G(\mathbf{x}) = \bar{G}(\mathbf{x})\mathrm{e}^{-\mathrm{i}\omega\left(\frac{M_\infty x}{c_\infty \beta_\infty^2} + \frac{\Phi_0'(\mathbf{x})}{c_\infty^2}\right)}. \tag{36}$$

Equations (35) and (36) give an explicit expression for the Green's function on the basis of Eq. (34), i.e.,

$$G(\mathbf{x}) = \frac{\exp\left[-\mathrm{i}k\left(\frac{\sqrt{x^2 + (1-M_\infty^2)(y^2+z^2)}}{\beta_\infty^2} + \frac{M_\infty x}{\beta_\infty^2} + \frac{\Phi_0'(\mathbf{x})}{c_\infty}\right)\right]}{4\pi\sqrt{x^2 + \beta_\infty^2(y^2+z^2)}}. \tag{37}$$

The above equation is extended to a generic source position (x_s, y_s, z_s), by writing

$$G(\mathbf{x}, \mathbf{x}_s) = \frac{\mathrm{e}^{-\mathrm{i}k\sigma_M}}{4\pi R_M} \tag{38}$$

where $\sigma_M = [R_M + M_\infty(x - x_s)]/\beta_\infty^2 + [\Phi_0'(\mathbf{x}) - \Phi_0'(\mathbf{x}_s)]/c_\infty$ is the generalized reverse flow phase radius, extending the definition given by Garrick and Watkins[24], and $R_M = \sqrt{(x - x_s)^2 + \beta_\infty^2[(y - y_s)^2 + (z - z_s)^2]}$ is the amplitude radius.

In the case of a uniform flow, Eq. (38) is equivalent to the solution provided by Wu and Lee[15]. On the other hand, for the reverse flow Taylor Green's function G_T, the terms depending on M_∞^2 are neglected in Eq. (38). It follows

$$G_T(\mathbf{x}, \mathbf{x}_s) = \frac{\mathrm{e}^{-\mathrm{i}k\sigma_{M_T}}}{4\pi R}, \tag{39}$$

where $\sigma_{M_T} = R + [\Phi_0(\mathbf{x}) - \Phi_0(\mathbf{x}_s)]/c_\infty$, $R = \sqrt{(x - x_s)^2 + (y - y_s)^2 + (z - z_s)^2}$ and Φ_0 denotes the total mean flow velocity potential.

V. INTEGRAL FORMULATION WITH SOURCE TERMS AND VARIATIONAL STATEMENT

Consider the weakly non-uniform potential flow Helmholtz equation with a generic distribution of sources $g(\mathbf{x}_s)$ in the domain Ω

$$k^2\phi - 2ik\mathbf{M}_0 \cdot \boldsymbol{\nabla}\phi + \nabla^2\phi - M_\infty^2 \frac{\partial^2\phi}{\partial x^2} = g(\mathbf{x}_s). \tag{40}$$

Following the same procedure adopted in Sec. III A, Eq. (11) is multiplied by ϕ and Eq. (40) by G. The difference of these equations integrated over the domain Ω is rewritten by using the divergence theorem to give

$$\begin{aligned} \hat{C}(\mathbf{x}_p)\phi(\mathbf{x}_p) = &\int_\Omega G(\mathbf{x}, \mathbf{x}_s) g(\mathbf{x}_s)\, dV \\ &+ \int_{\partial\Omega} \left[G\frac{\partial\phi}{\partial n} - \phi\frac{\partial G}{\partial n} - 2\mathrm{i}k\mathbf{M}_0 \cdot \mathbf{n} G\phi \right] dS \\ &- \int_{\partial\Omega} \left[M_\infty^2 \left(G\frac{\partial\phi}{\partial x} - \phi\frac{\partial G}{\partial x} \right) n_x \right] dS. \end{aligned} \tag{41}$$

where $G = G(\mathbf{x}_p, \mathbf{x})$ and $\phi = \phi(\mathbf{x})$ unless stated otherwise, $\mathbf{x} \in \partial\Omega$ and $\mathbf{x}_p$ is an arbitrary point either in Ω or on $\partial\Omega$. In the above expression $\mathbf{M}_0$ and $\mathbf{n}$ are given along the boundary surface $\partial\Omega$ (see Fig. 1).

Equation (41) can be solved numerically by means of a collocation BEM[15]. Alternatively, a variational formulation[25] can be defined. The major downside of a variational statement is the increase in computational cost due the double integration over the boundary surface. A variational statement of Eq. (41) is described below.

Equation (41) is rewritten observing that

$$\frac{\partial \phi}{\partial x} = \frac{\partial \phi}{\partial n}\frac{\partial n}{\partial x} + \frac{\partial \phi}{\partial \tau}\frac{\partial \tau}{\partial x} + \frac{\partial \phi}{\partial \eta}\frac{\partial \eta}{\partial x} = \frac{\partial \phi}{\partial n}n_x + \frac{\partial \phi}{\partial \tau}\tau_x + \frac{\partial \phi}{\partial \eta}\eta_x, \tag{42}$$

where τ and η indicate the coordinates along the unit tangent vectors $\boldsymbol{\tau}$ and $\boldsymbol{\eta}$ on $\partial\Omega$, such that the normal vector to the boundary is given by $\boldsymbol{n} = \boldsymbol{\tau} \times \boldsymbol{\eta}$. Substituting Eq. (42) into Eq. (41) yields:

$$\begin{aligned}
\hat{C}(\mathbf{x}_p)\phi(\mathbf{x}_p) &= \int_\Omega G(\mathbf{x}_p, \mathbf{x}_s) g(\mathbf{x}_s)\, dV \\
&+ \int_{\partial\Omega} \left[G\frac{\partial \phi}{\partial n} - \phi\frac{\partial G}{\partial n} - 2\mathrm{i}k\mathbf{M}_0 \cdot \mathbf{n} G\phi \right] dS \\
&- \int_{\partial\Omega} M_\infty^2 \left[G\left(\frac{\partial \phi}{\partial n}n_x + \frac{\partial \phi}{\partial \tau}\tau_x + \frac{\partial \phi}{\partial \eta}\eta_x \right) - \phi\frac{\partial G}{\partial x} \right] n_x dS.
\end{aligned} \tag{43}$$

Equation (43) is convenient from a computational point of view because the tangential derivative can be expressed as a sum of the shape functions multiplied by the nodal values of ϕ as shown by Wu and Lee[15]. Using a Galerkin approach, the residuals in Eq. (43) are required to be orthogonal to a test function $w(\mathbf{x}_p)$, giving

$$\begin{aligned}
\int_{\partial\Omega_{x_p}} \hat{C}(\mathbf{x}_p)\phi(\mathbf{x}_p) w^*(\mathbf{x}_p) dS_{x_p} &= \int_{\partial\Omega_{x_p}} \int_\Omega w^*(\mathbf{x}_p) G(\mathbf{x}_p, \mathbf{x}_s) g(\mathbf{x}_s)\, dV dS_{x_p} \\
&+ \int_{\partial\Omega x_p} \int_{\partial\Omega} w^*(\mathbf{x}_p) \left(G\frac{\partial \phi}{\partial n} - \phi\frac{\partial G}{\partial n} - 2\mathrm{i}k\mathbf{M}_0 \cdot \mathbf{n} G\phi \right) dS dS_{x_p} \\
&- \int_{\partial\Omega x_p} \int_{\partial\Omega} w^*(\mathbf{x}_p) M_\infty^2 \left[G\left(\frac{\partial \phi}{\partial n}n_x + \frac{\partial \phi}{\partial \tau}\tau_x + \frac{\partial \phi}{\partial \eta}\eta_x \right) - \phi\frac{\partial G}{\partial x} \right] n_x dS dS_{x_p},
\end{aligned} \tag{44}$$

where "*" indicates the complex conjugate.

Similarly, for the integral formulation associated with the Taylor transformation, Eq. (44) can be approximated by neglecting terms of order M_∞^2. Hence, using the Green's

function G_T yields:

$$\int_{\partial\Omega_{x_p}} C(\mathbf{x}_p)\phi(\mathbf{x}_p)w^*(\mathbf{x}_p)dS_{x_p} = \int_{\partial\Omega_{x_p}}\int_{\Omega} w^*(\mathbf{x}_p)G_T(\mathbf{x}_p,\mathbf{x}_s)g(\mathbf{x}_s)\ dVdS_{x_p}$$
$$+\int_{\partial\Omega_{x_p}}\int_{\partial\Omega} w^*(\mathbf{x}_p)\left(G_T\frac{\partial\phi}{\partial n}-\phi\frac{\partial G_T}{\partial n}-2\mathrm{i}k\mathbf{M}_0\cdot\mathbf{n}G_T\phi\right)dSdS_{x_p}. \tag{45}$$

VI. ERROR ESTIMATE

The weakly non-uniform potential flow wave equation, Eq. (6), is an approximation of the full potential linearized wave equation Eq. (1) accurate to the first order in M_0'. It is an exact formulation only for wave propagation on a uniform mean flow. This section presents a dimensional error analysis of the weakly non-uniform potential flow wave equation compared to the full potential linearized wave equation. If L_A and L_M are respectively the characteristic length scales associated with the acoustic field and with the mean flow field, Eq. (1) can be expressed in the frequency domain as follows:

$$\omega^2\phi - 2\mathrm{i}\omega\mathbf{u}_0\cdot\boldsymbol{\nabla}\phi + c_\infty^2\nabla^2\phi - u_\infty^2\frac{\partial^2\phi}{\partial x^2} = \tilde{E}(\phi), \tag{46}$$

where

$$\begin{aligned}\tilde{E} =&\mathbf{u}_0'\cdot\boldsymbol{\nabla}(\mathbf{u}_0'\cdot\boldsymbol{\nabla}\phi)+\mathbf{u}_\infty\cdot\boldsymbol{\nabla}(\mathbf{u}_0'\cdot\boldsymbol{\nabla}\phi)+\frac{1}{2}\boldsymbol{\nabla}\phi\cdot\boldsymbol{\nabla}(\mathbf{u}_0\cdot\mathbf{u}_0)\\ &+(\gamma-1)(\mathrm{i}\omega\phi+\mathbf{u}_0\cdot\boldsymbol{\nabla}\phi)\boldsymbol{\nabla}\cdot\mathbf{u}_0+\frac{\gamma-1}{2}(\|\mathbf{u}_0\|^2-\|\mathbf{u}_\infty\|^2)\nabla^2\phi.\end{aligned} \tag{47}$$

In Eq. (6) the terms on the l.h.s. of Eq. (46) are retained, whereas the terms included in the error function $\tilde{E}$ are dropped by assuming $M_0' \ll M_\infty$.

Following Astley and Bain[17], Eq. (47) is divided by c_∞^2 and the r.h.s. terms which

form $\tilde{E}(\phi)$ have the meaning indicated below:

$$\begin{aligned}
&\frac{1}{c_\infty^2}\mathbf{u}_0'\cdot\boldsymbol{\nabla}(\mathbf{u}_0'\cdot\boldsymbol{\nabla}\phi)\sim M_0'^2\frac{[\phi]}{L_AL_M},\\
&\frac{1}{c_\infty^2}\mathbf{u}_\infty\cdot\boldsymbol{\nabla}(\mathbf{u}_0'\cdot\boldsymbol{\nabla}\phi)\sim M_0'M_\infty\frac{[\phi]}{L_AL_M},\\
&\frac{1}{2}\boldsymbol{\nabla}\phi\cdot\boldsymbol{\nabla}(\mathbf{u}_0\cdot\mathbf{u}_0)\sim M_0'M_\infty\frac{[\phi]}{L_AL_M},\\
&\frac{1}{c_\infty^2}(\gamma-1)\boldsymbol{\nabla}\cdot\mathbf{u}_0\mathrm{i}\omega\phi\sim M_0'^3\frac{[\phi]}{L_AL_M},\\
&\frac{1}{c_\infty^2}(\gamma-1)(\boldsymbol{\nabla}\cdot\mathbf{u}_0)\mathbf{u}_0\cdot\boldsymbol{\nabla}\phi\sim M_0'^3M_\infty\frac{[\phi]}{L_AL_M},\\
&\frac{1}{c_\infty^2}\frac{\gamma-1}{2}(\|\mathbf{u}_0\|^2-\|\mathbf{u}_\infty\|^2)\nabla^2\phi\sim M_0'M_\infty\frac{[\phi]}{L_A^2}.
\end{aligned}\tag{48}$$

To correctly bound the error brought by the solution of Eq. (17), a combined Taylor-Lorentz transformation is applied to Eq. (46). In the transformed space, ϕ and G are exact solutions of the Helmholtz problem and the fundamental Helmholtz operator. Following the procedure described in Sec. IV to obtain Eq. (32), but considering the actual flow direction, Eq. (46) is transformed as follows:

$$\omega^2\phi+c_\infty^2\nabla_{\tilde{X}}^2\phi=\hat{E}_{\tilde{X}},\tag{49}$$

where

$$\hat{E}_{\tilde{X}}=\tilde{E}_{\tilde{X}}-\mathbf{u}_0'\cdot\mathbf{u}_0'\frac{\omega^2}{c_\infty^2\beta_\infty^2}\phi+2\frac{\mathrm{i}\omega}{\beta_\infty}(\boldsymbol{\nabla}_X\cdot\mathbf{u}_0')\phi.\tag{50}$$

The additional error terms are

$$\begin{aligned}
&\frac{1}{c_\infty^4}\mathbf{u}_0'\cdot\mathbf{u}_0'\frac{\omega^2}{c_\infty^2\beta_\infty^2}\phi\sim M_0'^2\frac{[\phi]}{L_A^2},\\
&\frac{1}{c_\infty^2}\frac{2\mathrm{i}\omega}{\beta_\infty}(\boldsymbol{\nabla}_X\cdot\mathbf{u}_0)\phi\sim M_0'^3\frac{[\phi]}{L_AL_M}.
\end{aligned}\tag{51}$$

Hence, from Eq. (50) the error associated with the weakly non-uniform potential flow wave equation is such that

$$\begin{aligned}
\hat{E}\sim\ &C_1\frac{M_0'M_\infty[\phi]}{L_AL_M}+C_2\frac{M_0'^2[\phi]}{L_AL_M}+C_3\frac{M_0'M_\infty[\phi]}{L_A^2}+C_4\frac{M_0'^2[\phi]}{L_A^2}+\\
&+C_5\frac{M_0'^3[\phi]}{L_AL_M}+C_6\frac{M_0'^3M_\infty[\phi]}{L_AL_M}.
\end{aligned}\tag{52}$$

where $C_1, C_2, .., C_6$ are constants of order 1.

From Eq. (52), the error $\hat{E}$ scales with $1/L_A = f/c_\infty$ where f is the frequency. In terms of mean flow length scale, the error varies with $1/L_M$. The error therefore decreases as the mean flow becomes more uniform. The error vanishes in a uniform flow ($M_0' = 0$). In other words, the accuracy of the formulation deteriorates only for propagation in a non-uniform region.

The error ε on the solution ϕ to Eq. (49) is obtained by convolving $\hat{E}$ with the Green's function G, i.e.,

$$\varepsilon(\mathbf{x}_p) = \int_\Omega G(\mathbf{x}_p, \mathbf{x}) \hat{E}(\mathbf{x}) \; dV(\mathbf{x}). \tag{53}$$

In the Taylor-Lorentz space G varies as $1/R_M$, where R_M is the amplitude radius of Eq. (38). Introducing the geometrical length scale D associated with the domain Ω, the above equation can be rewritten including Eqs. (48) and (51). The error contribution, ε_1, of the second and third terms in Eq. (48) to Eq. (53) is given by

$$\varepsilon_1 \sim [\phi] M_0^{'} M_\infty \frac{D}{L_M} \frac{D^2}{L_A R_M}. \tag{54}$$

The error ε_1 increases linearly with frequency. However, if $L_A R_M$ is constant, i.e. if the amplitude radius is inversely proportional to the wavelength, the error becomes independent of frequency.

This applies also to all the remaining terms in Eqs. (48) and (51) except for the error terms of order $1/L_A^2$. In this case, the last term of Eq. (48) produces an error, ε_2, in Eq. (53) that is given by

$$\varepsilon_2 \sim [\phi] M_0^{'} M_\infty D \frac{D^2}{L_A^2 R_M}. \tag{55}$$

Note that the above equation scales quadratically with frequency. The contribution of this term is significant only at high frequency.

Equations (54) and (55) can be rewritten by introducing the geometrical and acoustic relative distances of the observer, i.e. R_M/D and R_M/L_A, as

$$\varepsilon_1 = [\phi] M_0^{'} M_\infty \frac{D}{L_M} \left(\frac{D}{R_M}\right)^2 \frac{R_M}{L_A}, \qquad \varepsilon_2 = [\phi] M_0^{'} M_\infty \left(\frac{D}{R_M}\right)^3 \left(\frac{R_M}{L_A}\right)^2. \tag{56}$$

Small values of R_M/D denote the geometrical near field whereas large values of R_M/D are associated with the geometrical far field. Similar definitions can be given for the acoustic field on the basis of R_M/L_A. The above equations show that, when sound propagates in a

non-uniform flow, the error decreases in the geometrical far field but increases in the acoustical far field. Contours of ε_1 and ε_2 on a logarithmic scale are shown in Figs. 2a and 2b. The present error analysis can be extended to 2D problems, where G scales with $1/\sqrt{kR_M}$, but it is not explicitly reported here for the sake of conciseness.

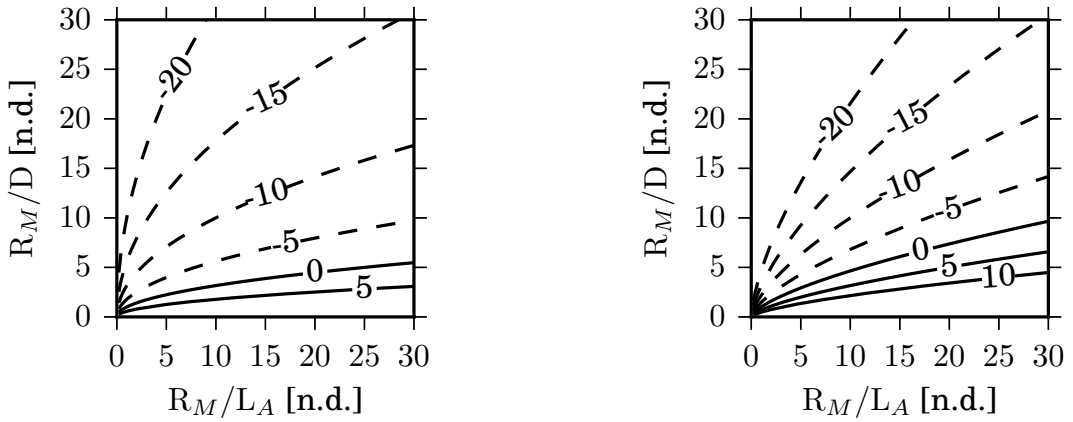

(a) ε_1 (dB)

(b) ε_2 (dB)

Figure 2: Contour of the error estimates, ε_1 and ε_2, on the weakly non-uniform potential flow equation Eq. (6) against the full potential linearized wave equation Eq. (1).

The same conclusion holds for the Taylor-Helmholtz formulation. However, the error increases even when wave propagation occurs on a uniform flow. This is because the Taylor-Helmholtz equation is also an approximation of the uniform flow convected Helmholtz equation, namely the error $\hat{E}$ does not vanish in a uniform flow region.

VII. BENCHMARK PROBLEM

In this section, numerical examples are provided to assess the accuracy of the boundary integral solution for the weakly non-uniform potential flow Helmholtz equation compared to a reference solution of the full potential linearized Helmholtz equation. A comparison with integral solutions for the uniform flow Helmholtz and the Taylor-Helmholtz equations is also provided.

First, the integral formulations are used to solve a 'wave extrapolation' problem where an 'inner' solution is obtained on an arbitrary closed surface in the flow and extrapolated to the far field by using the proposed integral formulation. Second, a traditional BEM

solution is presented in which the scattering from a point source by a rigid body is computed at all points external to the scatterer up to the boundary surface. In this study, the numerical issue associated with irregular frequencies in the BE solution is overcome by avoiding the characteristic frequencies of the scatterer.

The scattering by a rigid cylinder of radius a of the acoustic field generated by a monopole point source in a non-uniform mean flow is used as the basis for both the test cases. A full 2D problem is solved. The analytical solution of a potential inviscid incompressible mean flow around a cylinder is used to define the base mean flow and a monopole source of unit magnitude is defined at a point S. The problem is solved in an unbounded domain for far field Mach numbers in the range $0.0 \rightarrow 0.3$. The mean flow density $\rho_\infty = 1.22$ kg/m^3 and the speed of sound $c_\infty = 340$ m/s are constant. The reference pressure for the computation of the $SPL = 20\log_{10}(p_{rms}/p_{ref})$ is $p_{ref} = 2 \cdot 10^{-5}$ Pa.

As a reference solution, a Lagrangian FEM with cubic element interpolation based on 30 DoFs/λ is used to solve the full potential linearized wave equation Eq. (1). The problem is solved in the frequency domain and a perfectly matched layer (PML)[5] is applied to model the radiation condition. The PML is located at $r = 10a$. Due to the approximation of the source model and the radiation condition, an error of 0.05% at the outer surface of the computational domain is assessed to be present in the FE solution in the case of quiescent media.

A. Wave extrapolation test case

The first test case consists of a monopole source located at $x_s = (0, -1.5a)$ as shown in Fig. 3. In this case, the integral formulation is used to extrapolate the solution to the far field. First, the reference FE solution of the full potential linearized Helmholtz equation solves the radiation and scattering of a monopole source by the cylinder with a non-uniform flow in the inner domain Ω_{in}. Second, the reference solution is sampled on a closed control surface $\partial\Omega_{in}$, including the cylinder and the source, and radiated to the far field Ω_{out} by means of an integral formulation. In the current instance $\partial\Omega_{in}$ is located at a radial distance $r_{cs} = 2a$. The maximum value of M_0' on $\partial\Omega_{in}$ is $M_\infty/4$. The order of interpolation of the integral solution on Ω_{in} is consistent with the finite element model. The FE reference solution is also used as benchmark in the far field.

First, the error generated by the integral solution associated with the weakly non-uniform potential flow Helmholtz equation against the reference FE solution is calculated. The L^2 error is defined as

$$E_{L^2} = 100 \times \sqrt{\frac{\int_{\Gamma_{fp}} \|\phi(\mathbf{x}) - \phi(\mathbf{x})_{ref}\|^2 dS}{\int_{\Gamma_{fp}} \|\phi_{ref}(\mathbf{x})\|^2 dS}} \tag{57}$$

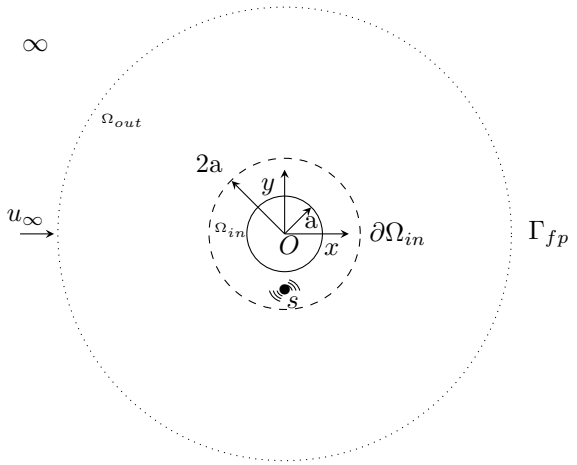

Figure 3: Geometry of reference for the wave extrapolation test case. Scattering by a cylinder from a monopole source on a potential mean flow. The sound field in the outer domain Ω_{out} is extrapolated based on the field on the inner surface $\partial\Omega_{in}$.

where Γ_{fp} denotes a closed circular arc of field points (see Fig. 3). The L^2 error for the acoustic velocity potential is shown in Fig. 4 plotted against the Helmholtz number, ka, on a circular arc of field points with radius $r_{fp} = 8a$. Note that the error is computed considering the physical distance of the observer R in lieu of the amplitude radius R_M since for $M_\infty \leq 0.3$ the maximum difference between R and R_M is about 3% of R. The variation of the L^2 error for ϕ against M_∞ is shown in Fig. 5 whereas the sensitivity of the L^2 error on the distance to the observer is shown in Fig. 6. In the latter, the error is computed on circular arcs of radii r_{fp} equal to $6a$, $8a$ and $10a$ for $ka = 4.25$. Note that the mean flow is almost uniform at these distances from the cylinder. To further assess the accuracy provided by the integral formulation for the weakly non-uniform potential flow Helmholtz equation, the computation of the L^2 error for ϕ against M_∞ is also performed for the formulation of Wu and Lee[15] and the Taylor-Helmholtz equation. This comparison is given in Fig. 7 at $r_{fp} = 8a$ plotted for different values of the the non-dimensional frequency ka.

A description of the local accuracy provided by the three integral formulations is presented in Fig. 8, which illustrates the pressure directivity at $r_{fp} = 8a$ for $ka = 9.24$ and $M_\infty = 0.3$ plotted against the angle θ, where $\theta = 0$ corresponds to the x-axis and θ is measured positive counterclockwise. The acoustic pressure is given by:

$$p = -\rho_0(\mathrm{i}\omega\phi + \mathbf{u}_0 \cdot \boldsymbol{\nabla}\phi). \tag{58}$$

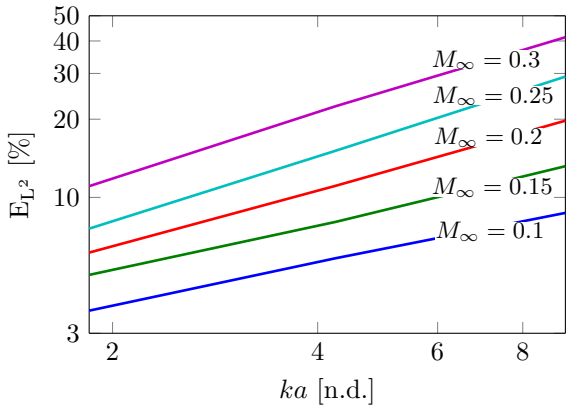

Figure 4: L^2 error for ϕ along a field point circular arc with radius $r_{fp} = 8a$ as a function of the non-dimensional frequency ka for the wave extrapolation test case of Fig. 3. The solution is based on the integral formulation for the weakly non-uniform potential flow Helmholtz equation Eq. (17).

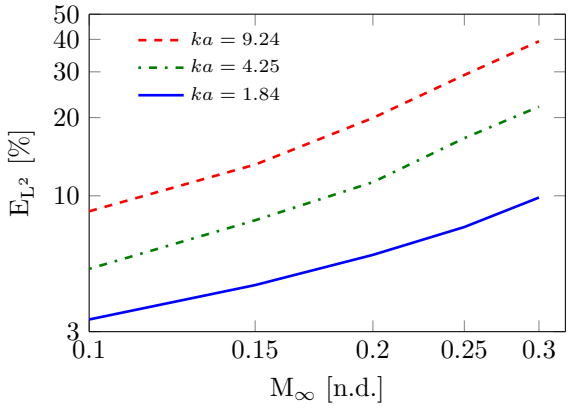

Figure 5: L^2 error for ϕ along a field point circular arc with radius $r_{fp} = 8a$ as a function of the mean flow Mach number M_∞ for the wave extrapolation test case of Fig. 3. The solution is based on the integral formulation for the weakly non-uniform potential flow Helmholtz equation Eq. (17).

Again, the FE solution of the full potential linearized Helmholtz equation is used as a reference result. The solution provided by the Taylor-Helmholtz equation introduces local

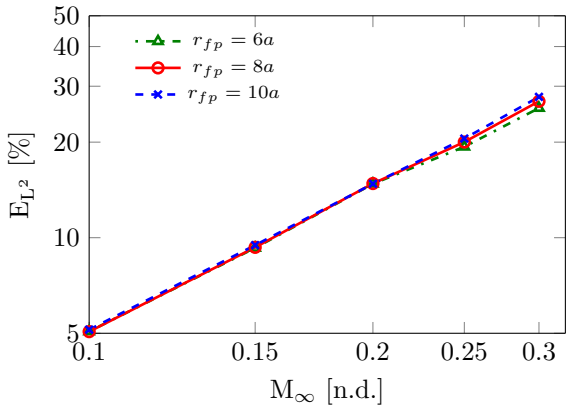

Figure 6: L^2 error for ϕ at $ka = 4.25$ along field point circular arcs with radii $r_{fp} = 6a, 8a$ and $10a$ as a function of the mean flow Mach number M_∞ for the wave extrapolation test case of Fig. 3. The solution is based on the integral formulation for the weakly non-uniform potential flow Helmholtz equation Eq. (17).

errors of up to 10 dB. On the other hand, the error given by the weakly non-uniform potential flow Helmholtz solution and the related uniform flow approximation is limited to 5 dB. However, the weakly non-uniform solution improves the results given by the uniform flow Helmholtz equation in the shielded area [$\theta = 60° - 120°$], where the mean flow is not aligned with the uniform stream.

The accuracy of the proposed integral formulation Eq. (17) decreases linearly with frequency (see Fig. 4) and increases linearly with M_∞ (see Fig. 5), whereas the error is almost constant when wave propagation occurs on a uniform mean flow (see Fig. 6) since the integral formulation associated with the weakly non-uniform potential flow Helmholtz equation is exact for a uniform base flow. These results validate the error analysis of Sec. VI.

Moreover, the integral formulation based on the weakly non-uniform potential flow Helmholtz equation provides the best accuracy independently of frequency and Mach number compared to the solution obtained using the integral formulations for the uniform flow Helmholtz and the Taylor-Helmhotlz equations (see Fig. 7). The non-uniform flow effects in the weakly non-uniform formulation improve the prediction made compared to the uniform flow Helmholtz equation. The Taylor formulation however performs poorly and is less accurate than the uniform flow formulation which assumes uniform flows at all points. The problem with the Taylor equation is that the error grows even in the uniform

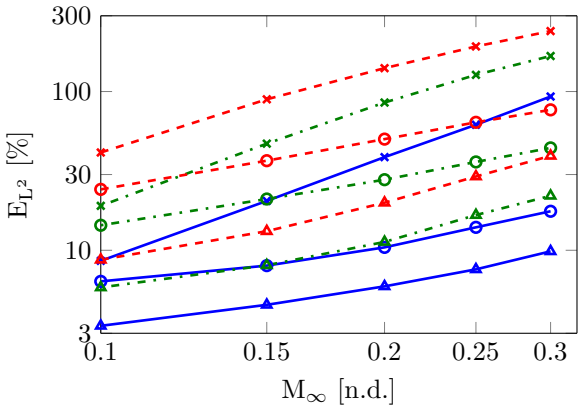

Figure 7: L^2 error for ϕ along a field point circular arc with radius $r_{fp} = 8a$ as a function of the mean flow Mach number M_∞ for the wave extrapolation test case of Fig. 3 at $ka = 1.84$ (solid), $ka = 4.25$ (dash) and $ka = 9.24$ (dash-dot). The solutions are based on the weakly non-uniform potential flow Helmholtz integral formulation Eq. (17) ($\triangle$), the uniform flow Helmholtz integral formulation[15] ($\circ$) and the Taylor-Helmholtz integral formulation Eq. (23) ($\times$).

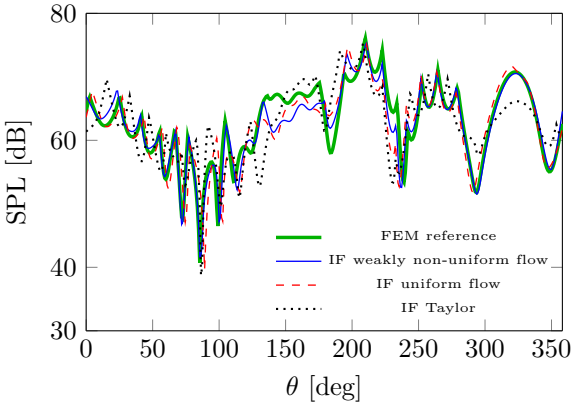

Figure 8: Acoustic pressure directivity along a field point circular arc with radius $r_{fp} = 8a$ for $ka = 9.24$ and $M_\infty = 0.3$. The wave extrapolation solution (see Fig. 3) is based on the integral formulations Eq. (17) (IF weakly non uniform), Wu and Lee[15] (IF uniform flow) and Eq. (23) (IF Taylor).

flow region whereas the uniform and the weakly non-uniform flow models are exact once this domain is reached.

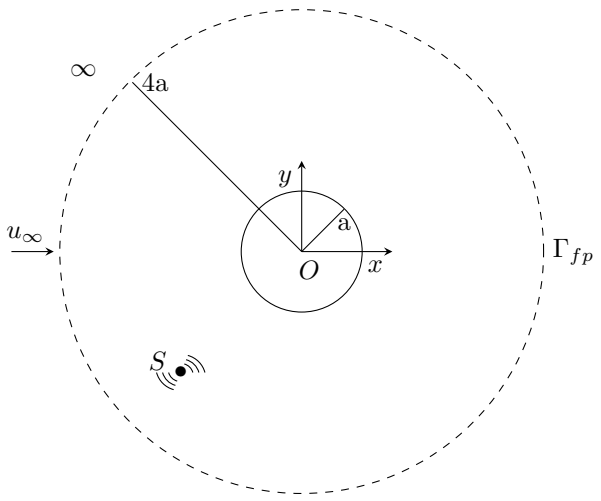

Figure 9: Reference domain for the BE solution. Scattering of a monopole source S by a rigid cylinder in an unbounded domain with non-uniform flow.

B. Boundary element test case

In this section, the accuracy of the boundary integral formulation for the weakly non-uniform potential flow Helmholtz equation is assessed by considering a direct BE solution of Eq. (44), solving for the surface acoustic velocity potential on the cylinder due to a point source scattering (see Fig. 9). The integral formulation is used to represent wave radiation and scattering up to the boundary surface, where the perturbations on the mean flow field M_0' are of the same order of magnitude of M_∞. The cylindrical scatterer with radius a is centered at the origin of the reference frame and a monopole source is located at $x_s = (-2a, -2a)$ as shown in Fig. 9. The error in the solution is calculated against the reference FE solution. A cubic Lagrangian BE interpolation with 10 DoFs/λ is used to solve the integral equations.

The dependency of the L^2 error for ϕ against frequency at a circular arc of field points with radius $r_{fp} = 4a$ is illustrated in Fig. 10. Again, note that the error is computed considering the physical distance of the observer, denoted previously as R, in lieu of R_M since for $M_\infty \leq 0.3$ the maximum difference between R and R_M is about 3% of R.

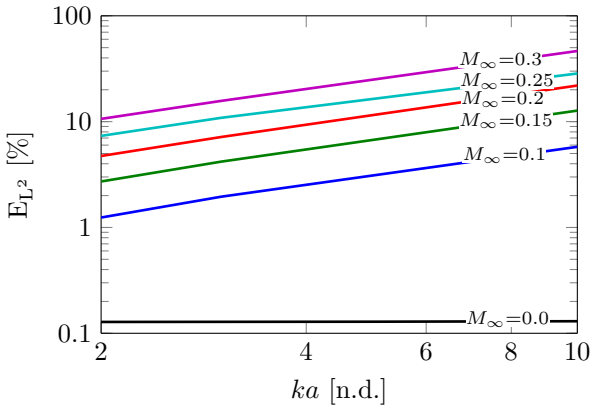

Figure 10: L^2 error for ϕ along a field point circular arc with radius $r_{fp} = 4a$ for the BE solution of the problem in Fig. 9 as a function of the non-dimensional frequency ka. The solution is based on Eq. (44).

Figure 11 shows the sensitivity of the L^2 error for ϕ to the distance of the observer sampling the error on circular arcs where the flow is almost uniform, for a non-dimensional

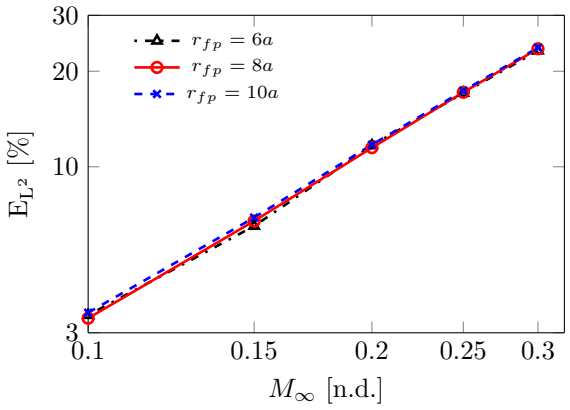

Figure 11: L^2 error for ϕ at a non-dimensional frequency $ka = 5$ along field point circular arcs with radii $r_{fp} = 6a, 8a$ and $10a$ for the BE solution of the problem in Fig. 9 as a function of the mean flow Mach number M_∞. The solution is based on Eq. (44).

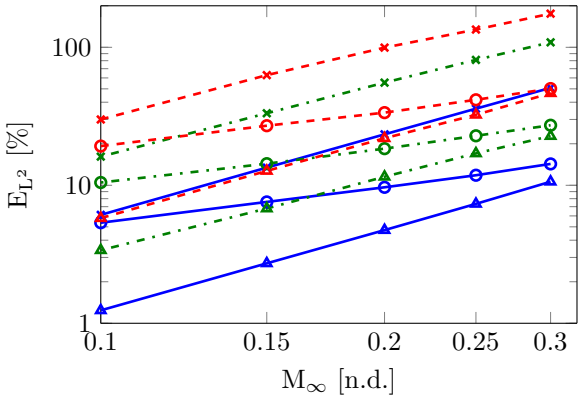

Figure 12: L^2 error for ϕ along a field point circular arc with radius $r_{fp} = 4a$ as a function of the mean flow Mach number M_∞ at non-dimensional frequencies $ka = 2$ (solid), $ka = 5$ (dash-dot) and $ka = 10$ (dash) for the problem in Fig. 9. The solutions are based on the weakly non-uniform potential flow Helmholtz equation Eq. (44) ($\triangle$), the uniform flow Helmholtz equation[15] ($\circ$) and the Taylor-Helmholtz equation Eq. (45) ($\times$).

frequency $ka = 5$. A comparison of the accuracy of the different integral solutions is also shown in Fig. 12 where the L^2 error for ϕ is computed at a field point arc with radius $r_{fp} = 4a$ for the weakly non-uniform potential flow Helmholtz equation, the uniform flow Helmholtz equation[15] and the Taylor-Helmholtz equation. Figures 13a, 13b and 13c show contours of the real part of ϕ over the solution domain for $ka = 10$ and $M_\infty = 0.3$. The weakly non-uniform potential flow formulation (Fig. 13a) clearly approximates the full potential FE solution (Fig. 13b) more accurately than the uniform flow Helmholtz solution (Fig. 13c). This is more evident if the sound source is in a region where the mean flow is strongly non-uniform, as shown in Fig. 14, where the same problem as in Fig. 9 is solved locating the monopole point source at $\mathbf{x}_s = (-1.3a, -0.5a)$.

The previous results have been presented in terms of computed value of the acoustic velocity potential. The acoustic pressure p is another quantity of practical interest. The absolute value of the acoustic pressure at $r_{fp} = 4a$ for $M_\infty = 0.1$ and 0.3 is shown in Figs. 15 and 16. The reference solution is compared to the approximate integral solutions at $ka = 10$ for different observer angular positions (the angle θ measured from the x-axis and positive counterclockwise). For $M_\infty = 0.1$, all of the integral formulations are mostly within 1 dB and 5 dB of the reference solution. However, at $M_\infty = 0.3$ the error incurred in the Taylor-Helmholtz solution reaches 10 dB. Nonetheless, the BEM prediction based on wave propagation on uniform flows underestimates the reference solution in the shielded

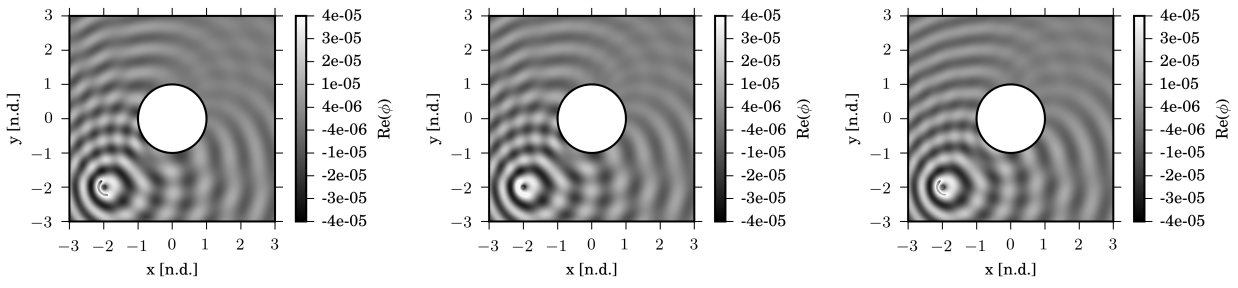

(a) (b) (c)

Figure 13: Real part of the acoustic velocity potential, $Re(\phi)$, at a non-dimensional frequency $ka = 10$ for $M_\infty = 0.3$. The BE solution of the weakly non-uniform potential flow Helmholtz equation (a), the FE solution of the full potential linearized Helmholtz equation (b) and the BE solution of the uniform flow Helmholtz equation[15] (c) are shown for the problem in Fig. 9.

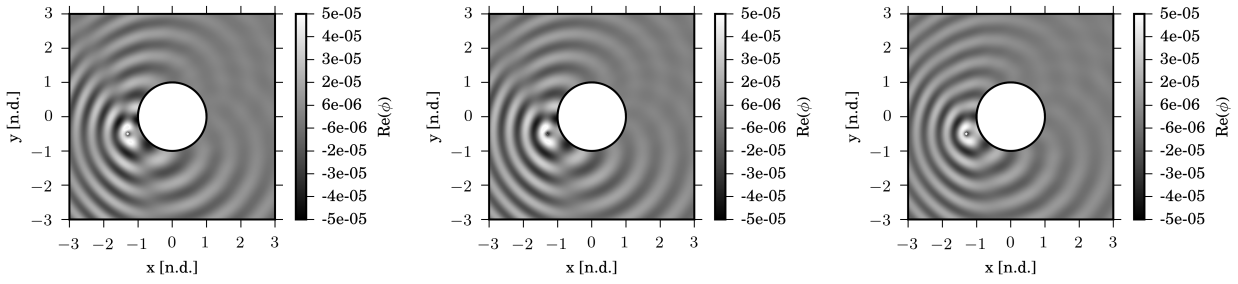

(a) (b) (c)

Figure 14: Real part of the acoustic velocity potential, $Re(\phi)$, at a non-dimensional frequency $ka = 10$ for $M_\infty = 0.3$. The BE solution of the weakly non-uniform potential flow Helmholtz equation (a), the FE solution of the full potential linearized Helmholtz equation (b) and the BE solution of the uniform flow Helmholtz equation[15] (c) are shown for the problem in Fig. 9 but locating a monopole point source at $\mathbf{x}_s = (-1.3a, -0.5a)$.

area $[\theta = 30^\circ - 90^\circ]$, where the incident and the scattered field interfere destructively and the flow is not aligned with the uniform stream. Note that the uniform flow Helmholtz formulation neglects wave refraction effects due to non-uniformities.

For the weakly non-uniform potential flow Helmholtz equation the error varies linearly with frequency (see Fig. 10) and with M_∞^2 (see Fig. 12). The error is independent of the observer distance when it is sampled on a region where the flow is almost uniform (see Fig. 11) because the formulation is exact for a uniform flow, namely no additional error is

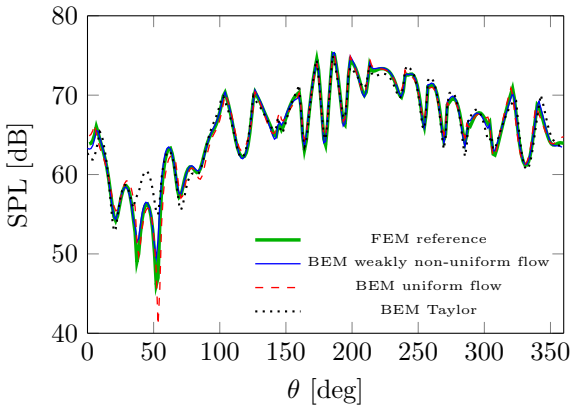

Figure 15: Acoustic pressure directivity along a field point circular arc with radius $r_{fp} = 4a$ at a non-dimensional frequency $ka = 10$ for a mean flow Mach number $M_\infty = 0.1$. The BE solutions (see Fig. 9) are based on the integral formulations Eq. (44) (BEM weakly non uniform), Wu and Lee [15] (BEM uniform flow) and Eq. (45) (BEM Taylor).

generated as the field point radius increases. These results validate further the error analysis of Sec. VI.

As in the previous test case, the weakly non-uniform flow Helmholtz formulation outperforms both the uniform flow Helmholtz and the Taylor-Helmholtz models (see Figs. 12, 15 and 16). The improvement against the uniform flow Helmholtz solution is larger at low Mach numbers. Since $M_0' \sim M_\infty$, for increasing M_∞ the error term of order $M_\infty M_0'/L_A^2$ in Eq. (48), becomes significant and increases the error of both the uniform and weakly non-uniform flow solutions at the same rate.

VIII. CONCLUDING REMARKS

A novel integral formulation for sound radiation on non-uniform mean flows has been proposed. It provides an approximate solution of the full potential linearized Helmholtz equation by assuming a weakly non-uniform potential mean flow. A Green's function, describing non-uniform flow effects on wave propagation, was derived for potential subsonic mean flows. The key advantage is that the Green's function and subsequent integral equation are presented in the physical space. The integral formulation is exact for wave propagation on a uniform flow and the error generated in the non-uniform flow region remains constant when wave propagation occurs on a uniform flow. This distinguishes the

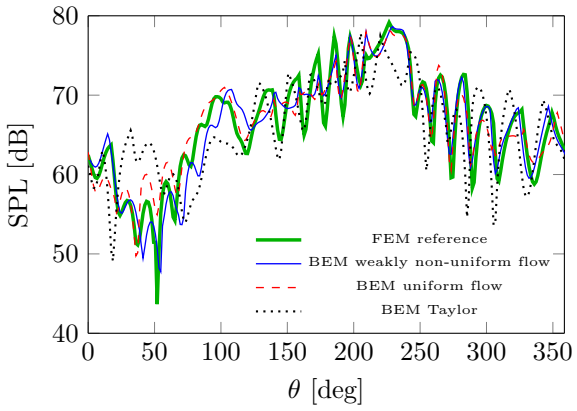

Figure 16: Acoustic pressure directivity along a field point circular arc with radius $r_{fp} = 4a$ at a non-dimensional frequency $ka = 10$ for a mean flow Mach number $M_\infty = 0.3$. The BE solutions (see Fig. 9) are based on the integral formulations Eq. (44) (BEM weakly non uniform), Wu and Lee [15] (BEM uniform flow) and Eq. (45) (BEM Taylor).

current approach from the *Taylor transformation* integral formulation applied by a number of previous researchers in computational Aeroacoustics [17,19,23].

A comparison with the Taylor integral formulation and the integral solution for the uniform flow Helmholtz equation (Lorentz formulation) has been presented. First, an analysis based on wave extrapolation on a non-uniform flow was performed. In this case, the condition that $M_0' \ll M_\infty$ was satisfied at all points outside the integral surface. For the weakly non-uniform potential flow Helmholtz solution the error varies linearly with M_∞ and is proportional to the frequency f. The new approach improves the accuracy over the Taylor formulation in which the error varies as M_∞^2 and is linear in f. It also outperforms the uniform flow Helmholtz equation, reducing the error of 40% for $M_\infty \leq 0.3$.

In a second test case the acoustic field was solved up to the solid scattering surface by means of a full BEM approach. On the boundary surface itself M_0' is of the same order of magnitude of M_∞, pushing to the limit the underlying assumption of the formulation of the analysis $M_0' \ll M_\infty$. An error analysis on the integral solution based on the weakly non-uniform potential flow Helmholtz equation shows that the L^2 error is proportional to M_∞^2 and varies linearly with f. A consistent improvement in accuracy is achieved against the integral solutions based on uniform mean flows and on the Taylor-Helmholtz equation for non-uniform flow. A significant advantage of the current weakly non-uniform potential

flow Helmholtz solution over the uniform flow Helmholtz solution is evident at low Mach numbers, where for instance a reduction of 50% of the error is observed at $M_\infty = 0.1$.

ACKNOWLEDGMENTS

The authors gratefully acknowledge the European Commission for the support of the project FP7-PEOPLE-2013-ITN CRANE, Grant Agreement 606844. The third author wishes to thank the Royal Commission for the Exhibition of 1851 for their outstanding support. Alastair Gregory kindly provided his results on the Taylor transformation to validate the Taylor-Helmholtz formulation.

APPENDIX A. INTEGRAL FORMULATION ON THE BOUNDARY SURFACE

An extension of Eq. (16) to the boundary surface is given on the basis of a limit approach[7], following Wu and Lee[15]. When an exterior wave propagation problem is considered, the domain Ω (see Fig. 1) is modified by subtracting a hemisphere of radius ϵ,

$$\begin{aligned}\phi(\mathbf{x}_p) = &\int_{\partial\Omega+\partial\Omega_\epsilon} \left(G\frac{\partial\phi}{\partial n} - \phi\frac{\partial G}{\partial n} \right) dS \\ &- \int_{\partial\Omega+\partial\Omega_\epsilon} \left[2\mathrm{i}k\mathbf{M}_0\cdot\mathbf{n}G\phi + M_\infty^2 \left(G\frac{\partial\phi}{\partial x} - \phi\frac{\partial G}{\partial x} \right) n_x \right] dS.\end{aligned} \tag{59}$$

When the radius ϵ tends to zero, the surface of the hemisphere tends to zero as ϵ^2. Since G varies as $1/\epsilon$, the contribution of the terms including G to the integral over the infinitesimal surface is zero. Hence, from Eq. (59),

$$\begin{aligned}\phi(\mathbf{x}_p) = &\int_{\partial\Omega} \left(G\frac{\partial\phi}{\partial n} - \phi\frac{\partial G}{\partial n} \right) dS \\ &- \int_{\partial\Omega} \left[2\mathrm{i}k\mathbf{M}_0\cdot\mathbf{n}G\phi + M_\infty^2 \left(G\frac{\partial\phi}{\partial x} - \phi\frac{\partial G}{\partial x} \right) n_x \right] dS \\ &- \phi(\mathbf{x}_p) \int_{\partial\Omega_\epsilon} \left(\frac{\partial G}{\partial n} - M_\infty^2\frac{\partial G}{\partial x}n_x \right) dS.\end{aligned} \tag{60}$$

In the limit of $\epsilon \to 0$ the Green's function in Eq. (11) tends to the Green's function of the static operator[15] G_0. The static operator associated with Eq. (11) is given by

$$\nabla^2 G_0 - M_\infty^2\frac{\partial^2 G_0}{\partial x^2} = \delta(\mathbf{x}-\mathbf{x}_s). \tag{61}$$

The solution of the equation above for a free field problem gives $G_0(\mathbf{x},\mathbf{x}_s) = 1/(4\pi R_M)$. Wu and Lee[15] have shown that the integral on the hemisphere of radius ϵ can be rewritten

on the boundary surface $\partial\Omega$ as follows:

$$\int_{\partial\Omega_\epsilon}\left(\frac{\partial G_0}{\partial n}-M_\infty^2\frac{\partial G_0}{\partial x}n_x\right)dS=-\int_{\partial\Omega}\left(\frac{\partial G_0}{\partial n}-M_\infty^2\frac{\partial G_0}{\partial x}n_x\right)dS. \tag{62}$$

Therefore, applying Eq. (62) to Eq. (60) yields

$$\begin{aligned}\hat{C}(\mathbf{x}_p)\phi(\mathbf{x}_p)=&\int_{\partial\Omega}\left(G\frac{\partial\phi}{\partial n}-\phi\frac{\partial G}{\partial n}\right)dS\\&-\int_{\partial\Omega}\left[2\mathrm{i}k\mathbf{M}_0\cdot\mathbf{n}G\phi+M_\infty^2\left(G\frac{\partial\phi}{\partial x}-\phi\frac{\partial G}{\partial x}\right)n_x\right]dS,\end{aligned} \tag{63}$$

where

$$\hat{C}(\mathbf{x}_p)=\begin{cases}1 & \mathbf{x}_p\in\Omega\\ 1-\int_{\partial\Omega}\left(\frac{\partial G_0}{\partial n}-M_\infty^2\frac{\partial G_0}{\partial x}n_x\right)dS & \mathbf{x}_p\in\partial\Omega\end{cases} \tag{64}$$

APPENDIX B. 2D GREEN'S FUNCTION

This section presents the 2D Green's function for wave propagation on a weakly non-uniform potential mean flow. The formulation is limited to subsonic flows. The solution is based on the proof given in Sec. IV. The Green's function for the Taylor-Helmholtz formulation is also derived.

The Green's function for the Helmholtz operator in the Taylor-Lorentz space, Eq. (33), is given by

$$G(\tilde{\mathbf{X}})=\frac{\mathrm{i}}{4\beta_\infty}H_0^{(2)}\left(\tilde{k}\tilde{R}_{2D}\right), \tag{65}$$

where $\tilde{R}_{2D}=\sqrt{\tilde{X}^2+\tilde{Y}^2}$, $H_0^{(2)}$ is the Hankel function of the second type of order zero and $\tilde{k}=k/\beta_\infty$. A time harmonic solution is sought for G, namely $G(\tilde{\mathbf{X}},\tilde{T})=G(\tilde{\mathbf{X}})e^{i\tilde{\omega}\tilde{T}}$. The inverse Taylor-Lorentz transformation is applied to the above equation retrieving the Green's function in the physical space, as described in Sec. IV,

$$G(\mathbf{x})=\frac{\mathrm{i}}{4\beta_\infty}H_0^{(2)}\left(\frac{k\sqrt{x^2+\beta_\infty^2y^2}}{\beta_\infty^2}\right)\mathrm{e}^{-\mathrm{i}k\left(\frac{M_\infty x}{\beta_\infty^2}+\frac{\Phi_0'(\mathbf{x})}{c_\infty}\right)}. \tag{66}$$

Extending the Green's function to a generic source position $\mathbf{x}_s=(x_s,y_s)$ yields

$$G(\mathbf{x})=\frac{\mathrm{i}}{4\beta_\infty}H_0^{(2)}\left(\frac{kR_{M,2D}}{\beta_\infty^2}\right)\mathrm{e}^{-\mathrm{i}k\left(\frac{M_\infty(x-x_s)}{\beta_\infty^2}+\frac{\Phi_0'(\mathbf{x})-\Phi_0'(\mathbf{x}_s)}{c_\infty}\right)} \tag{67}$$

where $R_{M,2D} = \sqrt{(x-x_s)^2 + \beta_\infty^2 (y-y_s)^2}$. The Green's function associated with the static operator Eq. (61) is $G_0 = -log(R_{M,2D})/2\pi$.

For a uniform flow, Eq. (67) reduces to the expression provided by Bailly and Juvé[26] including a reverse mean flow. On the other hand, if $M_\infty^2 \ll 1$, the 2D Green's function can be rewritten for the Taylor-Helmholtz formulation as

$$G_T(\mathbf{x}) = \frac{\mathrm{i}}{4\beta_\infty} H_0^{(2)}(kR_{2D}) \mathrm{e}^{-\mathrm{i}k\frac{\Phi_0(\mathbf{x})-\Phi_0(\mathbf{x}_s)}{c_\infty}} \tag{68}$$

where $R_{2D} = \sqrt{(x-x_s)^2 + (y-y_s)^2}$.

REFERENCES

1. R.J. Astley and W. Eversman, "Acoustic transmission in lined ducts with flow, part 2: the finite element method," *J. Sound and Vib.*, **74**, 103–121 (1981).

2. G. Gabard, "Discontinuous Galerkin methods with plane waves for time-harmonic problems," *J. Comput. Phys.*, **225**, 1961–1984 (2007).

3. C.K.W. Tam and J.C. Webb, "Dispersion-Relation-Preserving finite difference schemes for computational acoustics," *J. Comput. Phys.*, **107**, 262–281 (1993).

4. W. Eversman, "Mapped infinite wave envelope elements for acoustic radiation in a uniformly moving media," *J. Sound and Vib.*, **224**, 665–687 (1999).

5. A. Bermudez, L. Hervella-Nieto, A. Prieto and R. Rodriguez, "An optimal perfectly matched layer with unbounded absorbing function for time-harmonic acoustic scattering problems," *J. of Comput. Phys.*, **223**, 469–488 (2007).

6. I. Babuška and S. Sauter, " Is the pollution effect of the FEM avoidable for the Helmholtz equation considering high wave number?," *SIAM J. Numer. Anal.*, **34**, 2392–2423 (1997).

7. T.W. Wu (editor), *Boundary Element Acoustics: Fundamentals and computer codes*, (WIT Press, Southampton, 2000).

8. A. Delnevo, S. Le Saint, G. Sylvand and I. Terrasse, " Numerical methods: fast multipole method for shielding effects," *11th AIAA/CEAS Aeroac. Conf.* (Monterey, California), **AIAA 2005-3061**, (2005).

9. J.E. Ffowcs-Williams and D.L. Hawkings, "Sound generation by turbulence and surfaces in arbitrary motion," *Phil. Trans. R. Soc.*, **264A**, 321–342 (1969).

10. F. Farassat and M.K. Myers, "Extension of the Kirchhoff formula to radiation from moving surfaces," *J. Sound and Vib.*, **123**, 451–460 (1988).

11. C.J. Chapman, "Similarity variables for sound radiation in a uniform flow," *J. Sound and Vib.*, **233**, 157–164 (2000).

12. A. Gregory, S. Sinayoko, A. Agarwal and J. Lasenby, "An acoustic spacetime and the Lorentz transformation in aeroacoustics," *physics.flu-dyn*, **arXiv:1403.7511**, 1–28 (2014).

13. N. Balin, F. Casenave, F. Dubois, E. Duceau, S. Duprey and I. Terrasse, "Boundary element and finite element coupling for aeroacoustics simulations," *physics.comp-hp*, **arXiv:1402.2439**, 1–23 (2014).

14. F. Casenave, A. Ern and G. Sylvand, "Coupled BEM-FEM for the convected Helmholtz equation with non-uniform flow in a bounded domain," *J. Comput. Phys.*, **257**, 627–644 (2014).

15. T.W. Wu and L. Lee, "A direct boundary integral formulation for acoustics radiation in a subsonic uniform flow," *J. Sound and Vib.*, **175**, 51–63 (1994).

16. F.Q. Hu, "An efficient solution of time domain boundary integral equations for acoustic scattering and its acceleration by Graphics Processing Units," *19th AIAA/CEAS Aeroac. Conf.* (Berlin, Germany), **AIAA 2013-2018**, (2013).

17. R.J. Astley and J.G. Bain, "A 3D boundary element scheme for acoustic radiation in low Mach number," *J. Sound and Vib.*, **109**, 445–465 (1986).

18. K. Taylor, "A transformation of the acoustic equation with implications for wind-tunnel and low-speed flight tests," *Proc. R. Soc. London*, **65**, 125–136 (1979).

19. A. Agarwal and A.P. Dowling, "Low frequency acoustic shielding by the silent aircraft airframe," *AIAA J.*, **45**, 358–365 (2007).

20. A. Tinetti and M. Dunn, "Aeroacoustic noise prediction using the fast scattering code," *11th AIAA/CEAS Aeroac. Conf.* (Monterey, California), **AIAA 2005-3061**, (2005).

21. L. Lee, T.W. Wu and P. Zhang, "A dual-reciprocity method for acoustic radiation in a subsonic non-uniform flow," *Eng. Anal. Bound. Elem.*, **13**, 365–370 (1994).

22. R.J. Astley, "A finite element, wave envelope formulation for acoustical radiation in moving flows," *J. Sound and Vib.*, **103**, 471–485 (1985).

23. S. Mayoral and D. Papamoschou, "Prediction of jet noise shielding with forward flight effects," *51st AIAA Aerosp. Meet.* (Grapevin, Texas), **AIAA 2013-0010** (2013).

24. I.E. Garrick and C.E. Watkins, "A theoretical study of the effect of forward speed on the free-space sound-pressure field around propellers," *NACA* TN 3018, 1953.

25. H. Bériot, E. Perrey-Debain, M. Ben Tahar and C. Vayssade, "Plane wave basis in Galerkin BEM for bidimensional wave scattering," *Eng. Anal. Bound. Elem.*, **34**, 130–143 (2010).

26. C. Bailly, and D. Juvé, "Numerical solution of acoustic propagation problems using linearized Euler equations," *AIAA J.*, **38**, 22–28 (2000).